

# BIOREASON: Incentivizing Multimodal Biological Reasoning within a DNA-LLM Model

**Adibvafa Fallahpour**<sup>\*1,2,3,5</sup>

adibvafa.fallahpour@mail.utoronto.ca

**Andrew Magnuson**<sup>\*1,2</sup>

andrew.magnuson@mail.utoronto.ca

**Purav Gupta**<sup>\*1,2</sup>

purav.gupta@mail.utoronto.ca

**Shihao Ma**<sup>1,2,3</sup>

shihao.ma@mail.utoronto.ca

**Jack Naimer**<sup>1,2,3</sup>

jack.naimer@mail.utoronto.ca

**Arnav Shah**<sup>1,2,3</sup>

arnav.shah@mail.utoronto.ca

**Haonan Duan**<sup>1,2</sup>

haonan.duan@mail.utoronto.ca

**Omar Ibrahim**<sup>3</sup>

omar.ibrahim2@uhn.ca

**Hani Goodarzi**<sup>†4,6</sup>

hani.goodarzi@ucsf.edu

**Chris J. Maddison**<sup>†1,2,7</sup>

cmaddis@cs.toronto.edu

**Bo Wang**<sup>†1,2,3</sup>

bowang@vectorinstitute.ai

<sup>1</sup>University of Toronto <sup>2</sup>Vector Institute <sup>3</sup>University Health Network (UHN)

<sup>4</sup>Arc Institute <sup>5</sup>Cohere <sup>6</sup>University of California, San Francisco <sup>7</sup>Google DeepMind

## Abstract

Unlocking deep, interpretable biological reasoning from complex genomic data is a major AI challenge hindering scientific discovery. Current DNA foundation models, despite strong sequence representation, struggle with multi-step reasoning and lack inherent transparent, biologically intuitive explanations. We introduce BIOREASON, a pioneering architecture that, for the first time, deeply integrates a DNA foundation model with a large language model (LLM). This novel connection enables the LLM to directly process and reason with genomic information as a fundamental input, fostering a new form of multimodal biological understanding. BIOREASON’s sophisticated multi-step reasoning is developed through supervised fine-tuning and targeted reinforcement learning, guiding the system to generate logical, biologically coherent deductions. On biological reasoning benchmarks including KEGG-based disease pathway prediction—where accuracy improves from 88% to 97%—and variant effect prediction, BIOREASON demonstrates an average 15% performance gain over strong single-modality baselines. BIOREASON reasons over unseen biological entities and articulates decision-making through interpretable, step-by-step biological traces, offering a transformative approach for AI in biology that enables deeper mechanistic insights and accelerates testable hypothesis generation from genomic data. Data, code, and checkpoints are publicly available at <https://github.com/bowang-lab/BioReason>.

<sup>\*</sup>Equal contribution.

<sup>†</sup>Equal advising.

## 1 Introduction

Biological data—spanning genomics, transcriptomics, biomedical literature, and more—is expanding at an unprecedented rate, creating immense opportunities for scientific discovery. This data explosion has catalyzed the development of foundation models (FMs), deep networks trained on vast datasets that enable a wide array of downstream tasks. In genomics, DNA foundation models [5, 9, 24, 36, 12] have demonstrated remarkable capabilities by learning dense sequence representations that drive splice site identification, variant effect prediction, and regulatory element characterization.

Despite these advances, a critical challenge with foundation models still persists: effectively translating these learned representations into mechanistic insights and falsifiable hypotheses—the cornerstone of scientific advancement. Current DNA foundation models, while powerful in their representational capacity, typically function as "black boxes" that struggle with multi-step reasoning and lack the inherent ability to generate transparent, biologically intuitive explanations [3, 22]. These limitations become apparent in complex biological problems requiring mechanistic understanding, such as gene pathway analysis, phenotype prediction, and disease mechanism elucidation [8].

Large language models (LLMs) [25, 2, 11, 27] have rapidly advanced in reasoning capabilities, problem-solving, and knowledge depth. Through sophisticated training methods including reinforcement learning and supervised fine-tuning, these models demonstrate increasingly sophisticated multi-step reasoning across domains from mathematical problem-solving to logical deduction [13]. However, LLMs alone lack the specialized architecture to effectively process raw genomic sequences and often fail to capture nuanced biological patterns in genetic data.

This disconnect between powerful sequence representations of DNA foundation models and sophisticated reasoning capabilities of LLMs creates a significant barrier to developing AI systems that provide deep mechanistic insights comparable to biology domain experts. To bridge this gap, we present BIOREASON: a novel architecture that fundamentally integrates a DNA foundation model with an LLM, enabling a new paradigm of multimodal biological understanding and reasoning.

BIOREASON is distinguished by its ability to create a unique flow of information between genomic and natural language. This architecture enables the system to process raw DNA sequences while leveraging the reasoning capabilities of modern LLMs to generate biologically coherent explanations and predictions. Through a training methodology combining supervised fine-tuning and reinforcement learning, BIOREASON develops the capacity for sophisticated multi-step reasoning over genomic data—a capability that neither DNA foundation models nor LLMs can achieve independently.

**Contributions.** Our key contributions include:

- **Novel multimodal architecture.** The first successful integration of a DNA foundation model with an LLM, establishing a new methodology for AI-driven biological studies.
- **Advanced reasoning methodology.** A systematic training approach combining supervised fine-tuning and reinforcement learning that incentivizes multi-step biological reasoning.
- **New biological reasoning benchmarks.** Development and curation of novel benchmarks for evaluating biological reasoning capabilities, including an annotated reasoning dataset for gene pathway and disease prediction dataset from KEGG. [18]
- **Empirical performance improvements.** Demonstration that BIOREASON outperforms both DNA foundation models and LLMs used independently or in simple combination, with average performance gains of 15%+ over baseline.
- **Interpretable reasoning traces.** A mechanism for generating step-by-step biological reasoning traces that provide interpretable predictions, enhancing scientific insight and hypothesis generation

## 2 Background & Related Work

### 2.1 DNA Foundation Models

Recent years have witnessed the emergence of DNA foundation models [5, 9, 35, 24] that have significantly accelerated discovery throughout the biological sciences. These models extract meaningful representations directly from nucleotide sequences by pre-training on vast genomic datasets. Moreover, comprehensive benchmarking studies [14] have demonstrated their proficiency across various genomics tasks in both zero-shot and fine-tuned settings.

Evo2 [5], in particular, represents a significant advancement as one of the largest genomic foundation models to date, enabling extremely long-range context windows and predictions. Its ability to generate complete bacterial and yeast genomes underscores the potential of these models to capture complex genomic patterns. However, a critical limitation persists: these foundation models operate as "black boxes," lacking the interpretability necessary to explain how they derive conclusions from their embeddings. This opacity hampers the advancement of biological knowledge by obscuring the mechanistic insights that could otherwise be derived from model predictions.

## 2.2 Large Language Models for Biological Reasoning

LLMs have demonstrated remarkable capabilities in understanding and generating human-like text, with substantial success in interpreting and reasoning over complex biomedical data. Recent reviews [35] highlight their success across diverse domains, from clinical applications involving patient notes to biological research contexts. The development of specialized models pre-trained on biomedical literature [21], has further enhanced their domain-specific performance.

Genomics-focused LLMs such as GeneGPT [17] and agentic models such as TxGemma [32] represent initial attempts to integrate language models with genomic databases. However, these approaches primarily leverage pre-analyzed genomic data rather than directly interfacing with the raw sequence representations learned by DNA foundation models. Notably, no previous study has attempted to integrate these two paradigms—the textual knowledge encoded in LLMs and the sequence-level representations learned by DNA foundation models—into a unified framework capable of deep biological reasoning.

## 2.3 Genomics Benchmarks

DNA foundation models are typically evaluated on established benchmarks encompassing diverse prediction tasks, including regulatory element identification, variant effect prediction, transcription factor binding site prediction, and splice site classification. Comprehensive benchmarking frameworks like BEND [23] provide standardized evaluation protocols that enable meaningful comparisons between models across these supervised tasks.

While these benchmarks effectively measure performance on specific downstream applications, they inadequately evaluate a model's capacity for higher-order reasoning or hypothesis generation—capabilities essential for advancing scientific understanding. This represents a critical conceptual gap between current evaluation metrics and the sophisticated reasoning abilities desired from next-generation foundation models. The field requires benchmarks that challenge models to perform multi-step logical reasoning and predict potential biological mechanisms. This need motivated our curation of the KEGG pathway database to create a multi-step reasoning, variant effect prediction dataset that specifically evaluates a model's capacity for mechanistic biological reasoning.

## 3 BioReason Model

We introduce BIOREASON, a multimodal framework designed to unlock deep, interpretable biological reasoning by synergistically integrating genomic and language data. BIOREASON operates on two primary input streams: (i) one or more genomic sequences, denoted  $S_{\text{DNA}}$ ; and (ii) textual queries,  $Q_{\text{TEXT}}$ . These queries are processed by an LLM-specific tokenizer,  $T_{\text{LLM}}(\cdot)$ , into a sequence of  $M$  tokens  $(w_1, \dots, w_M)$  from the LLM's vocabulary  $\mathcal{V}_{\text{LLM}}$ . Current methods often fall short in this domain: Large Language Models (LLMs) treat  $S_{\text{DNA}}$  as simple strings, thereby missing rich genomic features, while DNA Foundation Models ( $f_{\text{DNA}}$ ) capture these features but primarily yield task-specific discriminative outputs (e.g., classification or regression scores) rather than interpretable natural language. BIOREASON bridges this gap by deriving contextualized DNA embeddings from the  $S_{\text{DNA}}$  input(s) and integrating them with the tokenized  $Q_{\text{TEXT}}$  to form a unified multimodal input sequence,  $X_{\text{LLM}}$ , for its core LLM. This direct integration enables the generation of explanatory text,  $Y_{\text{OUT}} = (y_1, \dots, y_K)$ , grounded in genomic nuances. The output  $Y_{\text{OUT}}$  presents biological reasoning and the final response. Figure 1 depicts the overall architecture.

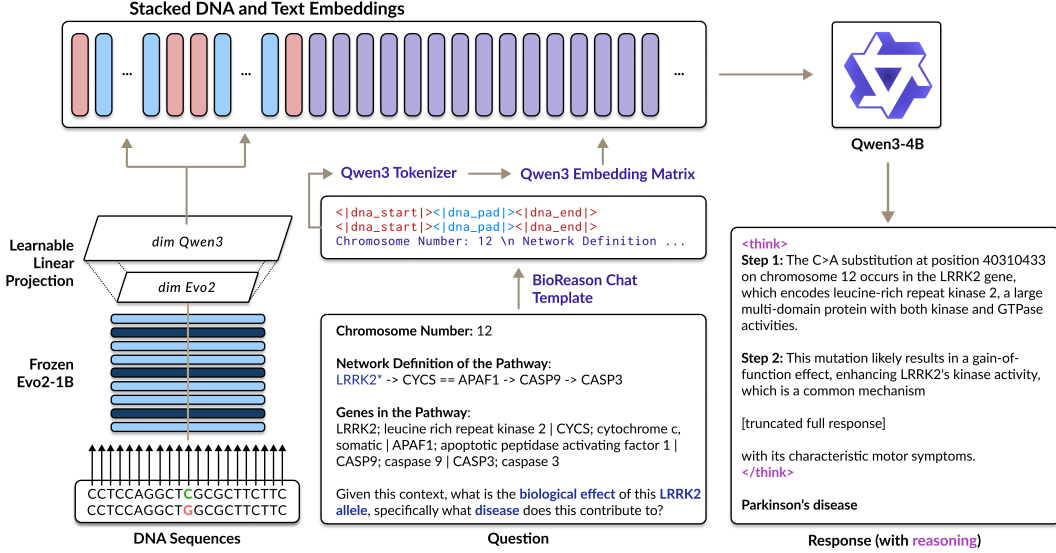


Figure 1: **BIOREASON Architecture**. Schematic representation of our novel multimodal framework that integrates a DNA foundation model with a Large Language Model.

### 3.1 DNA Foundation Model ( $f_{\text{DNA}}$ ) Encoder

$f_{\text{DNA}}$  transforms each input  $S_{\text{DNA}}$  sequence into contextualized embeddings. We utilize established DNA foundation models such as StripedHyena (e.g., Evo2) [5, 26], or the Nucleotide Transformer (NT), [10], as the  $f_{\text{DNA}}$ . Each  $S_{\text{DNA}}$  is first processed by its respective DNA-specific tokenizer,  $T_{\text{DNA}}(\cdot)$ , which segments it into a sequence of  $L'$  DNA tokens,  $D = (d_1, \dots, d_{L'})$ ; each token  $d_j$  can represent one or more nucleotides. If an input  $S_{\text{DNA}}$  sequence, after tokenization by  $T_{\text{DNA}}$ , exceeds a defined context length (e.g., 2048 DNA tokens), it is truncated. The chosen  $f_{\text{DNA}}$  architecture then maps each token sequence  $D$  to a sequence of high-dimensional per-token embeddings  $E_{\text{DNA}} = (e_1, \dots, e_{L'}) \in \mathbb{R}^{L' \times d_{\text{DNA}}}$ . These  $d_{\text{DNA}}$ -dimensional embeddings capture context-dependent genomic features. The weights of the  $f_{\text{DNA}}$  are kept frozen during BIOREASON’s training and inference.

### 3.2 Large Language Model ( $f_{\text{LLM}}$ ) Backbone

The  $f_{\text{LLM}}$  is the primary reasoning engine and text generator. We employ Qwen3 [33, 34], an autoregressive Transformer-based LLM, initialized with its original pre-trained weights. This model receives the multimodal input sequence  $X_{\text{LLM}}$  and is trained to predict the next token  $y_i$  in the sequence  $Y_{\text{OUT}}$ , conditioned on the preceding tokens  $y_{<i}$  and  $X_{\text{LLM}}$ . Mathematically, we optimize the parameters  $\theta_{\text{LLM}}$  of the  $f_{\text{LLM}}$  by maximizing the log-likelihood of the observed sequences:

$$\mathcal{L} = \sum_i \log P(y_i | y_{<i}, X_{\text{LLM}}; \theta_{\text{LLM}}) \quad (1)$$

The  $f_{\text{LLM}}$  utilizes special tokens to structure conversational interactions and reasoning within its textual output  $Y_{\text{OUT}}$ . These include tokens defining user and assistant roles (e.g., `<|im_start|>user/assistant ...<|im_end|>`), structuring reasoning steps (e.g., `<think> ...</think>`), alongside standard End-of-Sequence (EOS) and Padding (PAD) tokens.

### 3.3 Multimodal Genomic Integration

Genomic information, as DNA embeddings from  $f_{\text{DNA}}$ , is integrated into the  $f_{\text{LLM}}$ ’s input by stacking these with embeddings of the user’s query  $Q_{\text{TEXT}}$  and special tokens such as `<|dn_start|>` and `<|dn_end|>`. Key to this integration is the preparation of the DNA embedding block,  $E'_{\text{DNA}}$ , formed from one or more input DNA sequences. For each sequence  $S_{\text{DNA},k}$ , its  $f_{\text{DNA}}$ -generated embedding sequence  $E_{\text{DNA},k} \in \mathbb{R}^{L'_k \times d_{\text{DNA}}}$  (where  $L'_k$  is its tokenized length) is projected by a learnable linear layer,  $\text{Proj} : \mathbb{R}^{d_{\text{DNA}}} \rightarrow \mathbb{R}^{d_{\text{llm}}}$ , to yield  $E'_{\text{DNA},k}$  (of dimension  $d_{\text{llm}}$ ). The final  $E'_{\text{DNA}}$  block is a stack of these  $E'_{\text{DNA},k}$  sequences, with an embedded separator token  $e_{<\text{sep}>}$  interleaved between them.

Concurrently, the user’s tokenized query  $Q_{\text{TEXT}} = (w_1, \dots, w_M)$  is mapped to its embedding sequence  $\mathbf{E}_{Q_{\text{TEXT}}} = (E(w_1), \dots, E(w_M))$  by the  $f_{\text{LLM}}$ ’s input embedding layer,  $E(\cdot)$ . Similarly, the special tokens  $\langle \text{dna\_start} \rangle$ ,  $\langle \text{dna\_end} \rangle$ , and  $\langle \text{sep} \rangle$  are embedded via  $E(\cdot)$  to produce  $e_{\langle \text{dna\_start} \rangle}$ ,  $e_{\langle \text{dna\_end} \rangle}$ , and  $e_{\langle \text{sep} \rangle}$ , respectively. These embedding blocks are then stacked to form the multimodal input  $X_{\text{LLM}}$  for the  $f_{\text{LLM}}$ :

$$X_{\text{LLM}} = (e_{\langle \text{dna\_start} \rangle}, \mathbf{E}'_{\text{DNA}}, e_{\langle \text{dna\_end} \rangle}, \mathbf{E}_{Q_{\text{TEXT}}}) \quad (2)$$

All constituent embedding vectors within  $X_{\text{LLM}}$  receive positional information via Rotary Position Embedding (RoPE) [31], applied according to their final sequence positions. This strategy enables  $f_{\text{LLM}}$  fine-grained attention over both genomic and textual components within a unified modality.

### 3.4 Group Relative Policy Optimization (GRPO)

To further enhance BIOREASON’s reasoning performance beyond supervised fine-tuning, we employ Group Relative Policy Optimization (GRPO) [28, 11], a reinforcement learning strategy tailored for refining reasoning generation in language models. GRPO leverages reward signals within groups of sampled outputs, eliminating the need for an explicit value estimator.

For the full formalism, including the composite reward design, advantage normalization, and the clipped surrogate objective with KL regularization, please refer to Appendix A.4.

## 4 Datasets

To develop a multimodal DNA-LLM model with reasoning capabilities, we curated three datasets: one novel dataset specifically designed to incentivize reasoning and two adapted from established benchmarks. The adapted datasets are derived from ClinVar [20] and OMIM [1], which are widely used for variant effect prediction tasks. Our novel dataset is based on KEGG Network Variants data [18] and enhanced with cross-linked metadata from several public variant repositories including ClinVar [20], OMIM [1], dbSNP [29], and COSMIC [30]. This novel dataset relies on the high-quality manual annotations and descriptions from the curators of KEGG, for gene pathway descriptions and downstream phenotypic effects, like disease.

### 4.1 KEGG-Derived Biological Reasoning Dataset

#### 4.1.1 Dataset Integration and Statistics

We present a high-quality biological reasoning dataset derived from the Kyoto Encyclopedia of Genes and Genomes (KEGG) pathway database [18], consisting of 1,449 entries that elucidate the mechanistic connections between genetic variants and disease phenotypes. As seen in Figure 2, the dataset construction involved a rigorous multi-stage process that integrates structured pathway information with variant data to enable step-by-step reasoning across molecular networks.

For primary data integration, we extracted pathway network data from KEGG [18], focusing on disease-associated molecular interactions. Pathway data was augmented with variant information from clinical databases (ClinVar, dbSNP, OMIM, COSM) [20, 29, 1, 30] through a semi-automated mapping protocol [16, 19] that preserved relational integrity between genomic loci and functional elements within pathways. Each molecular network was represented using a standardized symbolic notation (e.g., "GENE1+GENE2 -> GENE3 -l GENE4") that encapsulates interaction types including activation, inhibition, complex formation, and transcriptional regulation.

To support variant interpretation, we included paired reference and variant sequences with precise alignment coordinates. These sequences have an average length of approximately 4,000 base pairs, with most variants differing by only 1–3 nucleotides from their reference sequences.

#### 4.1.2 Reasoning Path Construction and Curation

A distinctive feature of this dataset is its inclusion of explicit causal reasoning paths connecting genetic variants to disease phenotypes via defined molecular mechanisms; these paths were constructed using the Claude 3.7 Sonnet model [2] and grounded with contextual disease information from the KEGG disease database [18]. For training and evaluation, the dataset is structured into standardized

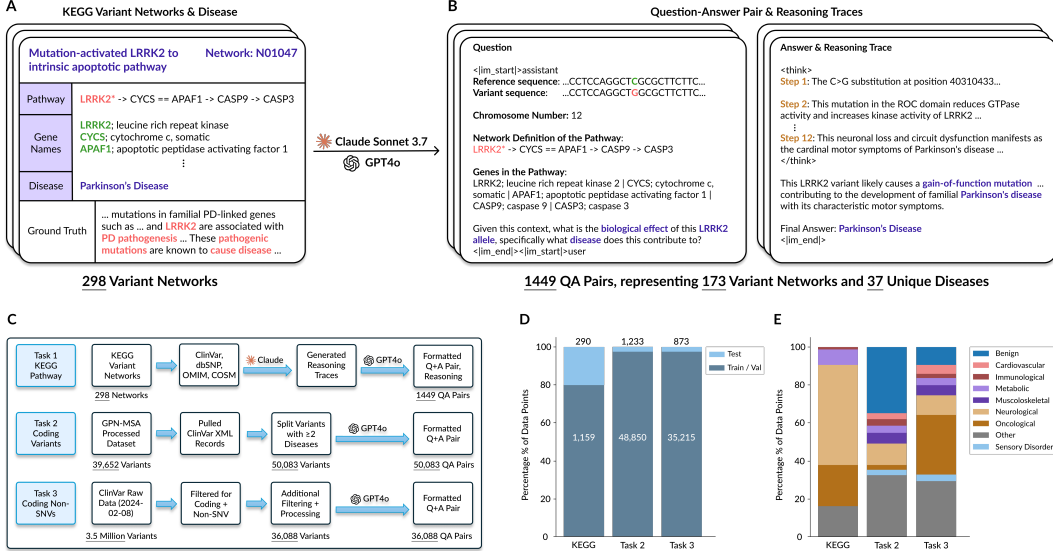


**Figure 2: BIOREASON Dataset Curation and Composition.** **A.** Representative example of a KEGG Variant Network element from the 298 networks utilized in our study, illustrating the relationship between genomic variants and their corresponding disease annotation that serves as ground truth for generating mechanistic reasoning traces. **B.** Exemplar of a structured question-answer pair with an accompanying multi-step reasoning trace demonstrating the expected logical progression from genomic variant to phenotypic outcome. **C.** Pipeline for data acquisition, integration, and curation across the three BIOREASON tasks. **D.** Distribution of train/test splits across the three curated datasets. 10% of train dataset was used for validation. **E.** Distribution of disease categories represented within the datasets, highlighting the diversity of variants and diseases represented in the datasets.

question-answer pairs: questions (illustrated in Figure 2B) incorporate variant details, network definitions, and gene descriptions, while answers provide concise mechanism-disease associations. The accompanying reasoning paths (mean length: 303.8 words) elaborate these mechanistic variant-to-phenotype links with precise molecular information.

## 4.2 Variant Effect Prediction of Coding Sequences

This dataset originated from the GPN-MSA [4] study. Affected gene names and disease phenotypes were extracted from ClinVar [20] XML records (via NCBI's Entrez Direct tool [19]), while benign variants were sourced from gnomAD v3.1.2 [7] (requiring allele number  $\geq 25,000$  and minor allele frequency (MAF)  $> 5\%$ ). The data was split by chromosome (Chr 1–7, 9–22, X, Y for training; Chr 8 for testing). For training augmentation, GPT-4o [25] generated 50 semantically equivalent question variations per sample, prompting for pathogenic/benign classification and conditional disease phenotype prediction using chromosome and gene context; mutations linked to multiple diseases were treated as distinct samples for comprehensive phenotype coverage.

## 4.3 Variant Effect Prediction of Coding Non-SNVs

Coding non-SNVs were sourced from the ClinVar [20] database (2024-02-28 release). We filtered variants to retain only coding non-SNVs within the nuclear genome, affecting  $\leq 64$  base pairs, of certain significance, and with a review status of at least two stars, matched to GRCh38.p14 transcripts. After extracting affected gene names and disease phenotypes where available, a custom algorithm partitioned the dataset to ensure balanced disease representation in train/test splits. Finally, to augment training data, GPT-4o [25] generated 50 semantically equivalent question variations for each entry, using gene and chromosome number as context, prompting for pathogenic/benign classification and, if pathogenic, the associated disease phenotype.

## 5 Experiments

### 5.1 Datasets

BIOREASON’s performance is evaluated on three datasets (detailed in Section 4):

**KEGG-Derived Biological Reasoning Dataset.** This dataset (1,449 variants, 37 unique diseases) evaluates multi-step mechanistic reasoning. Input: paired reference and variant DNA sequences ( $S_{DNA}$ ), and a textual query ( $Q_{TEXT}$ ) with pathway/gene context. Task: predict the mutation’s effect and resulting disease by sequence-to-sequence generation of  $Y_{OUT}$  containing step-by-step reasoning between `<think>` (special tokens) and the final disease.

**Variant Effect Prediction of Coding Sequences (VEP-Coding).** Comprising 50,083 core variant entries, this dataset tests classifying coding variants. Input: paired reference and variant DNA sequences ( $S_{DNA}$ ), and a textual query ( $Q_{TEXT}$ ) providing gene and chromosome context. Task: sequence generation to predict if a variant is benign, or pathogenic with its associated disease. Split: Chromosomes (Chr) 1–7, 9–22, X, Y for train/validation; Chr 8 for testing.

**Variant Effect Prediction of Coding Non-SNVs (VEP-Non-SNV).** Containing 36,088 core non-SNV entries, this dataset addresses non-SNV alterations (e.g., indels <64 bp). Input: paired reference and variant DNA sequences ( $S_{DNA}$ ), and an augmented textual query ( $Q_{TEXT}$ ) providing gene and chromosome context. Task: sequence generation to predict if a non-SNV is benign, or pathogenic with its associated disease(s). We used stratified train/test splits to ensure balanced disease representation.

### 5.2 Models and Baselines

To benchmark BIOREASON’s performance, we evaluated it against several baseline models, categorized as DNA foundation models ( $f_{DNA}$ ) and Large Language Models ( $f_{LLM}$ ).

For  $f_{DNA}$  baselines, we utilized pre-trained Evo2-1B [5] and Nucleotide Transformer (NT-500M) [10] models. For downstream predictions,  $f_{DNA}$  models were adapted with an attention head where a single learnable query vector attends to the sequence token embeddings to produce a final sequence representation. For ( $f_{LLM}$ ) baselines, we fine-tuned pre-trained Qwen3 models of two sizes: Qwen3-1.7B and Qwen3-4B [33, 34, 27]. These models were trained to receive text queries and DNA sequences treated as plain text strings and generate text with reasoning steps and final predictions.

The proposed BIOREASON models, were evaluated in several  $f_{DNA}$  and  $f_{LLM}$  combinations. Specifically, we tested Evo2-1B and NT-500M as  $f_{DNA}$  encoders, each paired with Qwen3-1.7B and Qwen3-4B as  $f_{LLM}$  backbones. The primary training methodology for all BIOREASON configurations was Supervised Fine-Tuning (SFT). Reinforcement Learning (RL) fine-tuning using the GRPO algorithm was subsequently applied to the NT-500M + Qwen3-1.7B (SFT+RL) model.

### 5.3 Experimental Setup

Our experimental setup varied by model architecture—BIOREASON, LLM-only, or  $f_{DNA}$ -only—and task. BIOREASON and LLM-only models underwent Supervised Fine-Tuning (SFT), with LLM parameters efficiently updated via Low-Rank Adaptation (LoRA) [15]. For  $f_{DNA}$ -only baselines, core DNA model weights were frozen; only a task-specific attention head and classifier were trained.

SFT objectives for these models differed: for the KEGG Dataset Task, models generated reasoning steps between ‘`<think>`’ tokens and a final disease prediction. For VEP Datasets Tasks, they aimed for pathogenic/benign classification and conditional disease prediction for pathogenic variants. During SFT, a specialized attention mask restricted loss computation exclusively to the response between ‘`<think>`’ tokens and final answer tokens, excluding those from the input query or DNA embeddings. Select BIOREASON models were further optimized with GRPO. Details for LoRA configurations, all SFT and RL hyperparameters, and GRPO reward functions are provided in Appendix A.1.

Performance evaluation metrics were task-specific. The KEGG Dataset Task utilized Accuracy, Macro F1-score, Macro Precision, and Macro Recall as a multi-class disease prediction assessment, considering potential class imbalances. For VEP Datasets Tasks, Accuracy and F1-score measured the binary pathogenic/benign classification. To ensure robust comparison, all LLM and DNA-LLM generations were deterministic with a decoding temperature of 0.

Table 1: Performance comparison of  $f_{\text{DNA}}$ -only, LLM-only, and DNA-LLM (BIOREASON) models on 290 test datapoints of the KEGG-derived biological reasoning task.

Model	Accuracy	F1-Score	Precision	Recall
[DNA] NT - 500M	86.55	69.76	73.23	66.61
[DNA] Evo2 - 1B	88.28	72.43	75.23	69.83
[LLM] Qwen3 - 1B	85.17	65.71	71.39	64.19
[LLM] Qwen3 - 4B	93.48	85.44	88.31	86.72
[DNA-LLM] NT + Qwen3 - 1B	88.42	72.13	75.42	71.91
[DNA-LLM] NT + Qwen3 - 1B (+RL)	89.66	74.11	78.82	72.96
[DNA-LLM] NT + Qwen3 - 4B	96.90	<b>89.03</b>	<b>90.99</b>	<b>89.38</b>
[DNA-LLM] Evo2 + Qwen3 - 1B	90.42	75.62	77.42	73.91
[DNA-LLM] Evo2 + Qwen3 - 4B	<b>97.24</b>	86.30	86.75	87.25

Table 2: Performance comparison of  $f_{\text{DNA}}$ -only, LLM-only, and DNA-LLM (BIOREASON) models on Variant Effect Prediction (VEP) benchmarks (VE-Coding with 1.23K and VE-Non-SNV with 873 test datapoints), evaluating pathogenic/benign classification.

Model	Variant Effect - Coding		Variant Effect - Non-SNV	
	Accuracy	F1-Score	Accuracy	F1-Score
[DNA] NT - 500M	60.91	45.20	67.93	65.97
[DNA] Evo2 - 1B	70.07	49.19	76.17	66.51
[LLM] Qwen3 - 1B	46.55	34.82	70.67	76.21
[LLM] Qwen3 - 4B	48.99	39.58	61.86	67.60
[DNA-LLM] NT + Qwen3 - 1B	55.58	54.50	72.82	76.93
[DNA-LLM] NT + Qwen3 - 4B	60.94	55.66	65.59	73.00
[DNA-LLM] Evo2 + Qwen3 - 1B	72.83	68.90	<b>88.20</b>	<b>89.91</b>
[DNA-LLM] Evo2 + Qwen3 - 4B	<b>80.21</b>	<b>80.00</b>	83.85	85.02

#### 5.4 Quantitative Results and Analysis

BIOREASON’s DNA-LLM hybrids deliver consistent, substantial gains over single-modality baselines across both mechanistic reasoning and variant effect tasks. On the KEGG-derived reasoning benchmark (Table 1), the Evo2+Qwen3-4B model achieves 97.24% accuracy and an 86.30% F1-score—outperforming the standalone Qwen3-4B LLM (93.48%/85.44%) and the Evo2 DNA-only model (88.28%/72.43%). Even with the smaller Qwen3-1B backbone, integrating DNA embeddings plus GRPO yields a boost from 88.42% to 89.66% accuracy and from 72.13% to 74.11% F1. On the VEP benchmarks (Table 2), the Evo2+Qwen3-4B hybrid attains 80.21% accuracy and 80.00% F1 in coding variant classification—well above DNA-only (70.07%/49.19%) and LLM-only (48.99%/39.58%)—while for non-SNV classification the Evo2+Qwen3-1B variant leads with 88.20% accuracy and an 89.91% F1, outstripping both DNA-only (76.17%/66.51%) and LLM-only (70.67%/76.21%) baselines.

#### 5.5 Case Study

To illustrate BIOREASON’s interpretable reasoning capabilities, consider a case where it was queried about the biological effect of a PFN1 allele on chromosome 17, given the pathway context ‘Actin(monomeric) // PFN1\* // Actin(filamentous)’. BIOREASON correctly predicted Amyotrophic Lateral Sclerosis (ALS) as the resultant disease. Significantly, the model generated a plausible 10-step mechanistic rationale, initiating by identifying a specific C>G substitution in the PFN1 gene. Its reasoning then connected this variant to profilin-1 dysfunction, impaired actin dynamics critical for cytoskeletal integrity, subsequent disruption of axonal transport in motor neurons, and finally, the motor neuron degeneration characteristic of ALS. This example highlights BIOREASON’s ability to not only make accurate predictions but also to articulate a step-by-step, biologically coherent pathway from a genomic variant to a complex disease phenotype.

	Question	Ground Truth (KEGG)	BioReason's Output
KEGG Data Point	<p>Question</p> <p>&lt; im_start &gt;user Chromosome Number: 17</p> <p>Network Definition of the Pathway: Actin(monomeric) // PFN1* // Actin(filamentous)</p> <p>Genes in the Pathway: ACTB; actin beta   ACTG1; actin gamma 1   PFN1; profilin 1</p> <p>Given this context, what is the <a href="#">biological effect</a> of this <a href="#">PFN1 allele</a>, specifically what <a href="#">disease</a> does this contribute to? &lt; im_end &gt;&lt; im_start &gt;assistant</p>	<p>Step 1: The variant KEGG_800 represents a C&gt;G substitution at position 4945969 on chromosome 17, occurring in the <b>PFN1</b> gene which encodes <b>profilin-1 protein</b>.</p> <p>Step 2: This nucleotide change ... potentially affecting a <b>functionally important domain</b>.</p> <p>⋮</p> <p>Step 10: The progressive loss of motor neurons results in <b>muscle weakness, atrophy</b>, and eventually <b>paralysis</b> - the hallmark clinical features of <b>ALS</b>.</p> <p>The C&gt;G mutation in the <b>PFN1</b> gene ... This cytoskeletal dysfunction contributes to <b>axonal transport defects</b> and <b>motor neuron degeneration</b>, ultimately leading to familial <b>Amyotrophic Lateral Sclerosis (ALS)</b>.</p>	<p>&lt;think&gt;</p> <p>... Step 3: This mutation likely <b>alters the protein structure or function of profilin-1</b>, potentially affecting its ability to bind actin monomers or regulate actin polymerization.</p> <p>⋮</p> <p>Step 10: This specific mutation contributes to ALS through a cytoskeletal/proteostasis pathway...</p> <p>This C&gt;G mutation in the <b>PFN1</b> gene <b>likely disrupts profilin-1 function</b>, impairing its ability to regulate actin dynamics by binding monomeric actin and promoting polymerization. The resulting cytoskeletal dysfunction affects motor neuron axonal transport and cellular homeostasis, contributing to the development of familial <b>amyotrophic lateral sclerosis (ALS)</b>.</p> <p>&lt;/think&gt;</p> <p>Answer: <b>amyotrophic lateral sclerosis (ALS)</b>&lt; im_end &gt;</p>

Figure 3: Case Study of BIOREASON’s Output

## 6 Discussion

BIOREASON successfully integrates DNA foundation models with large language models, enabling direct LLM reasoning on genomic data. This overcomes key limitations of opaque DNA models and the inability of LLMs to natively process DNA sequences, resulting in enhanced multi-step biological reasoning and superior predictive performance over single-modality approaches.

A core strength of BIOREASON is its interpretable reasoning. By processing contextualized DNA embeddings within the LLM, cultivated through supervised fine-tuning, the system provides not only accurate predictions but also articulates its decision-making via step-by-step mechanistic explanations formatted with ‘<think>’ tokens. This transparency is crucial, allowing researchers to scrutinize the model’s logic and translate computational outputs into testable scientific hypotheses.

The broader impact of this work lies in its potential to accelerate biological discovery. BIOREASON offers a robust tool for gaining deeper, mechanistic insights from genomic data, aiding in understanding complex disease pathways and the formulation of novel research questions. The development and application of benchmarks focused on multi-step reasoning, as utilized in this study, will further propel the advancement of AI systems capable of sophisticated biological understanding.

**Limitations.** Despite its strengths, BIOREASON has several limitations. First, reliance on curated datasets such as KEGG introduces potential biases and limits applicability to less-characterized genomic regions. Second, the computational overhead of encoding long DNA sequences and executing reinforcement learning fine-tuning (GRPO) increases both training and inference time, which may impede scalability to whole-genome analyses or real-time clinical workflows. Finally, while BIOREASON produces detailed reasoning paths, it currently lacks robust uncertainty quantification mechanisms, constraining its utility in high-stakes decision-making contexts.

**Future Work.** Future work will focus on expanding BIOREASON’s scope and applicability. Key directions include incorporating orthologous sequences to enhance data diversity and model generalizability, and adapting the core framework to other biological modalities such as RNA and protein sequences, thereby addressing a broader range of research questions. Additionally, BIOREASON’s improved variant effect prediction capabilities can be leveraged for impactful applications in genome-wide association studies (GWAS) and clinical mutation interpretation.

## 7 Conclusion

BIOREASON advances computational biology by seamlessly integrating high-capacity DNA sequence encoders with the flexible reasoning of large language models, yielding a unified framework that excels at both mechanistic pathway inference and variant pathogenicity prediction. Across KEGG-derived reasoning tasks and VEP benchmarks, our DNA–LLM hybrids consistently outperform models restricted to a single modality while generating transparent, stepwise explanations that facilitate expert validation. This tight multimodal fusion, further refined through reinforcement learning, not only boosts accuracy but also opens new avenues for interpretable genomic analysis. Future efforts will focus on tighter uncertainty calibration, leaner architectures for genome-scale deployment, and expansion into orthogonal data types—such as transcriptomes and proteomes—to broaden BIOREASON’s utility in precision medicine and biological discovery.

## References

- [1] J. Amberger, C. A. Bocchini, A. F. Scott, and A. Hamosh. Mckusick's online mendelian inheritance in man (omim®). *Nucleic Acids Research*, 37:D793, 2008. ISSN 03051048. doi: 10.1093/NAR/GKN665. URL <https://PMC2686440/>.
- [2] Anthropic. Claude 3.7 sonnet, February 2025. URL <https://www.anthropic.com/news/clause-3-7-sonnet>. Accessed: 2025-05-13.
- [3] G. Benegas, C. Ye, C. Albors, J. C. Li, and Y. S. Song. Genomic language models: Opportunities and challenges. *ArXiv*, page arXiv:2407.11435v2, 9 2024. ISSN 2331-8422. URL <https://PMC11275703/http://www.ncbi.nlm.nih.gov/articlerender.fcgi?artid=PMC11275703>.
- [4] G. Benegas, C. Albors, A. J. Aw, C. Ye, and Y. S. Song. A dna language model based on multispecies alignment predicts the effects of genome-wide variants. *Nature Biotechnology*, pages 1–6, 1 2025. ISSN 15461696. doi: 10.1038/S41587-024-02511-W;SUBJMETA=114, 1305,208,631;KWRD=GENETICS,MACHINE+LEARNING. URL <https://www.nature.com/articles/s41587-024-02511-w>.
- [5] G. Bixi, M. G. Durrant, J. Ku, M. Poli, G. Brockman, D. Chang, G. A. Gonzalez, S. H. King, D. B. Li, A. T. Merchant, M. Naghipourfar, E. Nguyen, C. Ricci-Tam, D. W. Romero, G. Sun, A. Taghibakshi, A. Vorontsov, B. Yang, M. Deng, L. Gorton, N. Nguyen, N. K. Wang, E. Adams, S. A. Baccus, S. Dillmann, S. Ermon, D. Guo, R. Ilango, K. Janik, A. X. Lu, R. Mehta, M. R. Mofrad, M. Y. Ng, J. Pannu, C. Ré, J. C. Schmok, J. S. John, J. Sullivan, K. Zhu, G. Zynda, D. Balsam, P. Collison, A. B. Costa, T. Hernandez-Boussard, E. Ho, M.-Y. Liu, T. McGrath, K. Powell, D. P. Burke, H. Goodarzi, P. D. Hsu, and B. L. Hie. Genome modeling and design across all domains of life with evo 2. *bioRxiv*, 2025. doi: 10.1101/2025.02.18.638918. URL <https://www.biorxiv.org/content/early/2025/02/21/2025.02.18.638918>.
- [6] W. Brown. Granular format rewards for eliciting mathematical reasoning capabilities in small language models. <https://gist.github.com/willccbb/4676755236bb08cab5f4e54a0475d6fb>. GitHub Gist.
- [7] S. Chen, L. C. Francioli, J. K. Goodrich, R. L. Collins, M. Kanai, Q. Wang, J. Alföldi, N. A. Watts, C. Vittal, L. D. Gauthier, T. Poterba, M. W. Wilson, Y. Tarasova, W. Phu, R. Grant, M. T. Yohannes, Z. Koenig, Y. Farjoun, E. Banks, S. Donnelly, S. Gabriel, N. Gupta, S. Ferriera, C. Tolonen, S. Novod, L. Bergelson, D. Roazen, V. Ruano-Rubio, M. Covarrubias, C. Llanwarne, N. Petrillo, G. Wade, T. Jeandet, R. Munshi, K. Tibbets, M. Abreu, C. A. A. Salinas, T. Ahmad, C. M. Albert, D. Ardiissino, I. M. Armean, E. G. Atkinson, G. Atzman, J. Barnard, S. M. Baxter, L. Beaugerie, E. J. Benjamin, D. Benjamin, M. Boehnke, L. L. Bonnycastle, E. P. Bottinger, D. W. Bowden, M. J. Bown, H. Brand, S. Brant, T. Brookings, S. Bryant, S. E. Calvo, H. Campos, J. C. Chambers, J. C. Chan, K. R. Chao, S. Chapman, D. I. Chasman, R. Chisholm, J. Cho, R. Chowdhury, M. K. Chung, W. K. Chung, K. Cibulskis, B. Cohen, K. M. Connolly, A. Correa, B. B. Cummings, D. Dabelea, J. Danesh, D. Darbar, P. Darnowsky, J. Denny, R. Duggirala, J. Dupuis, P. T. Ellinor, R. Elosua, J. Emery, E. England, J. Erdmann, T. Esko, E. Evangelista, D. Fatkin, J. Florez, A. Franke, J. Fu, M. Färkkilä, K. Garimella, J. Gentry, G. Getz, D. C. Glahn, B. Glaser, S. J. Glatt, D. Goldstein, C. Gonzalez, L. Groop, S. Gudmundsson, A. Haessly, C. Haiman, I. Hall, C. L. Hanis, M. Harms, M. Hiltunen, M. M. Holi, C. M. Hultman, C. Jalas, M. Kallela, D. Kaplan, J. Kaprio, S. Kathiresan, E. E. Kenny, B. J. Kim, Y. J. Kim, D. King, G. Kirov, J. Kooner, S. Koskinen, H. M. Krumholz, S. Kugathasan, S. H. Kwak, M. Laakso, N. Lake, T. Langsford, K. M. Laricchia, T. Lehtimäki, M. Lek, E. Lipscomb, R. J. Loos, W. Lu, S. A. Lubitz, T. T. Luna, R. C. Ma, G. M. Marcus, J. Marrugat, K. M. Mattila, S. McCarroll, M. I. McCarthy, J. L. McCauley, D. McGovern, R. McPherson, J. B. Meigs, O. Melander, A. Metspalu, D. Meyers, E. V. Minikel, B. D. Mitchell, V. K. Mootha, A. Naheed, S. Nazarian, P. M. Nilsson, M. C. O'Donovan, Y. Okada, D. Ongur, L. Orozco, M. J. Owen, C. Palmer, N. D. Palmer, A. Palotie, K. S. Park, C. Pato, A. E. Pulver, D. Rader, N. Rahman, A. Reiner, A. M. Remes, D. Rhodes, S. Rich, J. D. Rioux, S. Ripatti, D. M. Roden, J. I. Rotter, N. Sahakian, D. Saleheen, V. Salomaa, A. Saltzman, N. J. Samani, K. E. Samocha, A. Sanchis-Juan, J. Scharf, M. Schleicher, H. Schunkert, S. Schönherr, E. G. Seaby, S. H. Shah, M. Shand, T. Sharpe, M. B. Shoemaker, T. Shyong, E. K. Silverman, M. Singer-Berk, P. Sklar, J. T. Smith, J. G. Smith, H. Soininen, H. Sokol, R. G. Son, J. Soto, T. Spector,

C. Stevens, N. O. Stitzel, P. F. Sullivan, J. Suvisaari, E. S. Tai, K. D. Taylor, Y. Y. Teo, M. Tsuang, T. Tuomi, D. Turner, T. Tusie-Luna, E. Vartiainen, M. Vawter, L. Wang, A. Wang, J. S. Ware, H. Watkins, R. K. Weersma, B. Weisburd, M. Wessman, N. Whiffin, J. G. Wilson, R. J. Xavier, A. O'Donnell-Luria, M. Solomonson, C. Seed, A. R. Martin, M. E. Talkowski, H. L. Rehm, M. J. Daly, G. Tiao, B. M. Neale, D. G. MacArthur, and K. J. Karczewski. A genomic mutational constraint map using variation in 76,156 human genomes. *Nature* 2023 625:7993, 625:92–100, 12 2023. ISSN 1476-4687. doi: 10.1038/s41586-023-06045-0. URL <https://www.nature.com/articles/s41586-023-06045-0>.

[8] M. E. Consens, B. Li, A. R. Poetsch, and S. Gilbert. Genomic language models could transform medicine but not yet. *npj Digital Medicine*, 8:1–4, 12 2025. ISSN 23986352. doi: 10.1038/S41746-025-01603-4;SUBJMETA=1538,692,700;KWRD=HEALTH+CARE, HEALTH+POLICY. URL <https://www.nature.com/articles/s41746-025-01603-4>.

[9] H. Dalla-Torre, L. Gonzalez, J. Mendoza-Revilla, N. L. Carranza, A. H. Grzywaczewski, F. Oteri, C. Dallago, E. Trop, B. P. de Almeida, H. Sirelkhatim, G. Richard, M. Skwark, K. Beguir, M. Lopez, and T. Pierrot. Nucleotide transformer: building and evaluating robust foundation models for human genomics. *Nature Methods*, 22:287–297, 2 2024. ISSN 15487105. doi: 10.1038/S41592-024-02523-Z;SUBJMETA=114,1305,1647,208,212,631,794;KWRD=GENOMICS,MACHINE+LEARNING,SOFTWARE. URL <https://www.nature.com/articles/s41592-024-02523-z>.

[10] H. Dalla-Torre, L. Gonzalez, J. Mendoza-Revilla, N. Lopez Carranza, A. H. Grzywaczewski, F. Oteri, C. Dallago, E. Trop, B. P. De Almeida, H. Sirelkhatim, G. Richard, M. Skwark, K. Beguir, M. Lopez, and T. Pierrot. Nucleotide transformer: building and evaluating robust foundation models for human genomics. *Nature Methods*, 22(2):287–297, Feb. 2025. ISSN 1548-7091, 1548-7105. doi: 10.1038/s41592-024-02523-z. URL <https://www.nature.com/articles/s41592-024-02523-z>.

[11] DeepSeek-AI, D. Guo, D. Yang, H. Zhang, J. Song, R. Zhang, R. Xu, Q. Zhu, S. Ma, P. Wang, X. Bi, X. Zhang, X. Yu, Y. Wu, Z. F. Wu, Z. Gou, Z. Shao, Z. Li, Z. Gao, A. Liu, B. Xue, B. Wang, B. Wu, B. Feng, C. Lu, C. Zhao, C. Deng, C. Zhang, C. Ruan, D. Dai, D. Chen, D. Ji, E. Li, F. Lin, F. Dai, F. Luo, G. Hao, G. Chen, G. Li, H. Zhang, H. Bao, H. Xu, H. Wang, H. Ding, H. Xin, H. Gao, H. Qu, H. Li, J. Guo, J. Li, J. Wang, J. Chen, J. Yuan, J. Qiu, J. Li, J. L. Cai, J. Ni, J. Liang, J. Chen, K. Dong, K. Hu, K. Gao, K. Guan, K. Huang, K. Yu, L. Wang, L. Zhang, L. Zhao, L. Wang, L. Zhang, L. Xu, L. Xia, M. Zhang, M. Zhang, M. Tang, M. Li, M. Wang, M. Li, N. Tian, P. Huang, P. Zhang, Q. Wang, Q. Chen, Q. Du, R. Ge, R. Zhang, R. Pan, R. Wang, R. J. Chen, R. L. Jin, R. Chen, S. Lu, S. Zhou, S. Chen, S. Ye, S. Wang, S. Yu, S. Zhou, S. Pan, S. S. Li, S. Zhou, S. Wu, S. Ye, T. Yun, T. Pei, T. Sun, T. Wang, W. Zeng, W. Zhao, W. Liu, W. Liang, W. Gao, W. Yu, W. Zhang, W. L. Xiao, W. An, X. Liu, X. Wang, X. Chen, X. Nie, X. Cheng, X. Liu, X. Xie, X. Liu, X. Yang, X. Li, X. Su, X. Lin, X. Q. Li, X. Jin, X. Shen, X. Chen, X. Sun, X. Wang, X. Song, X. Zhou, X. Wang, X. Shan, Y. K. Li, Y. Q. Wang, Y. X. Wei, Y. Zhang, Y. Xu, Y. Li, Y. Zhao, Y. Sun, Y. Wang, Y. Yu, Y. Zhang, Y. Shi, Y. Xiong, Y. He, Y. Piao, Y. Wang, Y. Tan, Y. Ma, Y. Liu, Y. Guo, Y. Ou, Y. Wang, Y. Gong, Y. Zou, Y. He, Y. Xiong, Y. Luo, Y. You, Y. Liu, Y. Zhou, Y. X. Zhu, Y. Xu, Y. Huang, Y. Li, Y. Zheng, Y. Zhu, Y. Ma, Y. Tang, Y. Zha, Y. Yan, Z. Z. Ren, Z. Ren, Z. Sha, Z. Fu, Z. Xu, Z. Xie, Z. Zhang, Z. Hao, Z. Ma, Z. Yan, Z. Wu, Z. Gu, Z. Zhu, Z. Liu, Z. Li, Z. Xie, Z. Song, Z. Pan, Z. Huang, Z. Xu, Z. Zhang, and Z. Zhang. Deepseek-r1: Incentivizing reasoning capability in llms via reinforcement learning. 1 2025. URL <https://arxiv.org/pdf/2501.12948.pdf>.

[12] A. Fallahpour, V. Gureghian, G. J. Filion, A. B. Lindner, and A. Pandi. Codontransformer: A multispecies codon optimizer using context-aware neural networks. *Nature Communications*, 16(1), Apr 2025. doi: 10.1038/s41467-025-58588-7.

[13] A. Fallahpour, J. Ma, A. Munim, H. Lyu, and B. Wang. Medrax: Medical reasoning agent for chest x-ray, 2025. URL <https://arxiv.org/abs/2502.02673>.

[14] H. Feng, L. Wu, B. Zhao, C. Huff, J. Zhang, J. Wu, L. Lin, P. Wei, C. Wu, P. W. pwei, and A. Professor. Benchmarking dna foundation models for genomic sequence classification running title: Dna foundation models benchmarking. doi: 10.1101/2024.08.16.608288. URL <https://doi.org/10.1101/2024.08.16.608288>.

[15] E. J. Hu, Y. Shen, P. Wallis, Z. Allen-Zhu, Y. Li, S. Wang, L. Wang, and W. Chen. Lora: Low-rank adaptation of large language models, 2021. URL <https://arxiv.org/abs/2106.09685>.

[16] E. Huckvale and H. N. Moseley. kegg pull: a software package for the restful access and pulling from the kyoto encyclopedia of gene and genomes. *BMC Bioinformatics*, 24:1–17, 12 2023. ISSN 14712105. doi: 10.1186/S12859-023-05208-0/TABLES/12. URL <https://bmcbioinformatics.biomedcentral.com/articles/10.1186/s12859-023-05208-0> <http://creativecommons.org/publicdomain/zero/1.0/>.

[17] Q. Jin, Y. Yang, Q. Chen, and Z. Lu. Genegpt: augmenting large language models with domain tools for improved access to biomedical information. *Bioinformatics*, 40, 2 2024. ISSN 13674811. doi: 10.1093/BIOINFORMATICS/BTAE075. URL <https://dx.doi.org/10.1093/bioinformatics/btae075>.

[18] M. Kanehisa, M. Furumichi, Y. Sato, Y. Matsuura, and M. Ishiguro-Watanabe. Kegg: biological systems database as a model of the real world. *Nucleic Acids Research*, 53:D672–D677, 1 2025. ISSN 0305-1048. doi: 10.1093/NAR/GKAE909. URL <https://dx.doi.org/10.1093/nar/gkae909>.

[19] J. Kans. Entrez direct: E-utilities on the unix command line - entrez programming utilities help - ncbi bookshelf, 4 2013. URL <https://www.ncbi.nlm.nih.gov/books/NBK179288/>.

[20] M. J. Landrum, J. M. Lee, G. R. Riley, W. Jang, W. S. Rubinstei, D. M. Church, and D. R. Magogt. Clinvar: Public archive of relationships among sequence variation and human phenotype. *Nucleic Acids Research*, 42, 1 2014. ISSN 03051048. doi: 10.1093/NAR/GKT1113,. URL <https://pubmed.ncbi.nlm.nih.gov/24234437/>.

[21] J. Lee, W. Yoon, S. Kim, D. Kim, S. Kim, C. H. So, and J. Kang. Biobert: a pre-trained biomedical language representation model for biomedical text mining. *Bioinformatics*, 36: 1234–1240, 2 2020. ISSN 1367-4803. doi: 10.1093/BIOINFORMATICS/BTZ682. URL <https://dx.doi.org/10.1093/bioinformatics/btz682>.

[22] Q. Li, Z. Hu, Y. Wang, L. Li, Y. Fan, I. King, G. Jia, S. Wang, L. Song, and Y. Li. Progress and opportunities of foundation models in bioinformatics. *Briefings in Bioinformatics*, 25:548, 9 2024. ISSN 14774054. doi: 10.1093/BIB/BBAE548. URL <https://dx.doi.org/10.1093/bib/bbae548>.

[23] F. I. Marin, F. Teufel, M. Horlacher, D. Madsen, D. Pultz, O. Winther, and W. Boomsma. Bend: Benchmarking dna language models on biologically meaningful tasks. *12th International Conference on Learning Representations, ICLR 2024*, 11 2023. URL <https://arxiv.org/pdf/2311.12570.pdf>.

[24] E. Nguyen, M. Poli, M. Faizi, A. W. Thomas, C. B. Sykes, M. Wornow, A. Patel, C. Rabideau, S. Massaroli, Y. Bengio, S. Ermon, S. A. Baccus, and C. Ré. Hyenadna: Long-range genomic sequence modeling at single nucleotide resolution. *ArXiv*, 6 2023. ISSN 2331-8422. URL <https://arxiv.org/pdf/2306.15794.pdf>.

[25] OpenAI, : A. Hurst, A. Lerer, A. P. Goucher, A. Perelman, A. Ramesh, A. Clark, A. Ostrow, A. Welihinda, A. Hayes, A. Radford, A. Mądry, A. Baker-Whitcomb, A. Beutel, A. Borzunov, A. Carney, A. Chow, A. Kirillov, A. Nichol, A. Paino, A. Renzin, A. T. Passos, A. Kirillov, A. Christakis, A. Conneau, A. Kamali, A. Jabri, A. Moyer, A. Tam, A. Crookes, A. Tootoochian, A. Tootoonchian, A. Kumar, A. Vallone, A. Karpathy, A. Braunstein, A. Cann, A. Codispoti, A. Galu, A. Kondrich, A. Tulloch, A. Mishchenko, A. Baek, A. Jiang, A. Pelisse, A. Woodford, A. Gosalia, A. Dhar, A. Pantuliano, A. Nayak, A. Oliver, B. Zoph, B. Ghorbani, B. Leimberger, B. Rossen, B. Sokolowsky, B. Wang, B. Zweig, B. Hoover, B. Samic, B. McGrew, B. Spero, B. Giertler, B. Cheng, B. Lightcap, B. Walkin, B. Quinn, B. Guaraci, B. Hsu, B. Kellogg, B. Eastman, C. Lugaresi, C. Wainwright, C. Bassin, C. Hudson, C. Chu, C. Nelson, C. Li, C. J. Shern, C. Conger, C. Burette, C. Voss, C. Ding, C. Lu, C. Zhang, C. Beaumont, C. Halacy, C. Koch, C. Gibson, C. Kim, C. Choi, C. McLeavey, C. Hesse, C. Fischer, C. Winter, C. Czarnecki, C. Jarvis, C. Wei, C. Koumouzelis, D. Sherburn, D. Kappler, D. Levin, D. Levy, D. Carr, D. Farhi, D. Mely, D. Robinson, D. Sasaki, D. Jin, D. Valladares, D. Tsipras, D. Li, D. P.

Nguyen, D. Findlay, E. Oiwoh, E. Wong, E. Asdar, E. Proehl, E. Yang, E. Antonow, E. Kramer, E. Peterson, E. Sigler, E. Wallace, E. Brevdo, E. Mays, F. Khorasani, F. P. Such, F. Raso, F. Zhang, F. von Lohmann, F. Sulit, G. Goh, G. Oden, G. Salmon, G. Starace, G. Brockman, H. Salman, H. Bao, H. Hu, H. Wong, H. Wang, H. Schmidt, H. Whitney, H. Jun, H. Kirchner, H. P. de Oliveira Pinto, H. Ren, H. Chang, H. W. Chung, I. Kivlichan, I. O’Connell, I. O’Connell, I. Osband, I. Silber, I. Sohl, I. Okuyucu, I. Lan, I. Kostrikov, I. Sutskever, I. Kanitscheider, I. Gulrajani, J. Coxon, J. Menick, J. Pachocki, J. Aung, J. Betker, J. Crooks, J. Lennon, J. Kiros, J. Leike, J. Park, J. Kwon, J. Phang, J. Teplitz, J. Wei, J. Wolfe, J. Chen, J. Harris, J. Varavva, J. G. Lee, J. Shieh, J. Lin, J. Yu, J. Weng, J. Tang, J. Yu, J. Jang, J. Q. Candela, J. Beutler, J. Landers, J. Parish, J. Heidecke, J. Schulman, J. Lachman, J. McKay, J. Uesato, J. Ward, J. W. Kim, J. Huizinga, J. Sitkin, J. Kraaijveld, J. Gross, J. Kaplan, J. Snyder, J. Achiam, J. Jiao, J. Lee, J. Zhuang, J. Harriman, K. Fricke, K. Hayashi, K. Singhal, K. Shi, K. Karthik, K. Wood, K. Rimbach, K. Hsu, K. Nguyen, K. Gu-Lemberg, K. Button, K. Liu, K. Howe, K. Muthukumar, K. Luther, L. Ahmad, L. Kai, L. Itow, L. Workman, L. Pathak, L. Chen, L. Jing, L. Guy, L. Fedus, L. Zhou, L. Mamitsuka, L. Weng, L. McCallum, L. Held, L. Ouyang, L. Feuvrier, L. Zhang, L. Kondraciuk, L. Kaiser, L. Hewitt, L. Metz, L. Doshi, M. Aflak, M. Simens, M. Boyd, M. Thompson, M. Dukhan, M. Chen, M. Gray, M. Hudnall, M. Zhang, M. Aljubeh, M. Litwin, M. Zeng, M. Johnson, M. Shetty, M. Gupta, M. Shah, M. Yatbaz, M. J. Yang, M. Zhong, M. Glaese, M. Chen, M. Janner, M. Lampe, M. Petrov, M. Wu, M. Wang, M. Fradin, M. Pokrass, M. Castro, M. O. T. de Castro, M. Pavlov, M. Brundage, M. Wang, M. Khan, M. Murati, M. Bavarian, M. Lin, M. Yesildal, N. Soto, N. Gimelshein, N. Cone, N. Staudacher, N. Summers, N. LaFontaine, N. Chowdhury, N. Ryder, N. Stathas, N. Turley, N. Tezak, N. Felix, N. Kudige, N. Keskar, N. Deutsch, N. Bundick, N. Puckett, O. Nachum, O. Okelola, O. Boiko, O. Murk, O. Jaffe, O. Watkins, O. Godement, O. Campbell-Moore, P. Chao, P. McMillan, P. Belov, P. Su, P. Bak, P. Bakkum, P. Deng, P. Dolan, P. Hoeschele, P. Welinder, P. Tillet, P. Pronin, P. Tillet, P. Dhariwal, Q. Yuan, R. Dias, R. Lim, R. Arora, R. Troll, R. Lin, R. G. Lopes, R. Puri, R. Miyara, R. Leike, R. Gaubert, R. Zamani, R. Wang, R. Donnelly, R. Honsby, R. Smith, R. Sahai, R. Ramchandani, R. Huet, R. Carmichael, R. Zellers, R. Chen, R. Chen, R. Nigmatullin, R. Cheu, S. Jain, S. Altman, S. Schoenholz, S. Toizer, S. Miserendino, S. Agarwal, S. Culver, S. Ethersmith, S. Gray, S. Grove, S. Metzger, S. Hermani, S. Jain, S. Zhao, S. Wu, S. Jomoto, S. Wu, Shuaiqi, Xia, S. Phene, S. Papay, S. Narayanan, S. Coffey, S. Lee, S. Hall, S. Balaji, T. Broda, T. Stramer, T. Xu, T. Gogineni, T. Christianson, T. Sanders, T. Patwardhan, T. Cunningham, T. Degry, T. Dimson, T. Raoux, T. Shadwell, T. Zheng, T. Underwood, T. Markov, T. Sherbakov, T. Rubin, T. Stasi, T. Kaftan, T. Heywood, T. Peterson, T. Walters, T. Eloundou, V. Qi, V. Moeller, V. Monaco, V. Kuo, V. Fomenko, W. Chang, W. Zheng, W. Zhou, W. Manassra, W. Sheu, W. Zaremba, Y. Patil, Y. Qian, Y. Kim, Y. Cheng, Y. Zhang, Y. He, Y. Zhang, Y. Jin, Y. Dai, and Y. Malkov. Gpt-4o system card. 10 2024. URL <https://arxiv.org/pdf/2410.21276.pdf>.

- [26] M. Poli, J. Wang, S. Massaroli, J. Quesnelle, R. Carlow, E. Nguyen, and A. Thomas. Striped-Hyena: Moving Beyond Transformers with Hybrid Signal Processing Models, 12 2023. URL <https://github.com/togethercomputer/stripedhyena>.
- [27] Qwen, :, A. Yang, B. Yang, B. Zhang, B. Hui, B. Zheng, B. Yu, C. Li, D. Liu, F. Huang, H. Wei, H. Lin, J. Yang, J. Tu, J. Zhang, J. Yang, J. Yang, J. Zhou, J. Lin, K. Dang, K. Lu, K. Bao, K. Yang, L. Yu, M. Li, M. Xue, P. Zhang, Q. Zhu, R. Men, R. Lin, T. Li, T. Tang, T. Xia, X. Ren, X. Ren, Y. Fan, Y. Su, Y. Zhang, Y. Wan, Y. Liu, Z. Cui, Z. Zhang, and Z. Qiu. Qwen2.5 technical report. 12 2024. URL <https://arxiv.org/pdf/2412.15115.pdf>.
- [28] Z. Shao, P. Wang, Q. Zhu, R. Xu, J. Song, X. Bi, H. Zhang, M. Zhang, Y. K. Li, Y. Wu, and D. Guo. Deepseekmath: Pushing the limits of mathematical reasoning in open language models, 2024. URL <https://arxiv.org/abs/2402.03300>.
- [29] S. T. Sherry, M. H. Ward, M. Kholodov, J. Baker, L. Phan, E. M. Smigelski, and K. Sirotnik. dbSNP: the NCBI database of genetic variation. *Nucleic Acids Research*, 29:308–311, 1 2001. ISSN 0305-1048. doi: 10.1093/NAR/29.1.308. URL <https://dx.doi.org/10.1093/nar/29.1.308>.
- [30] Z. Sondka, N. B. Dhir, D. Carvalho-Silva, S. Jupe, Madhumita, K. McLaren, M. Starkey, S. Ward, J. Wilding, M. Ahmed, J. Argasinska, D. Beare, M. S. Chawla, S. Duke, I. Fasanella, A. G. Neogi, S. Haller, B. Hetenyi, L. Hodges, A. Holmes, R. Lyne, T. Maurel, S. Nair, H. Pedro,

A. Sangrador-Vegas, H. Schuilenburg, Z. Sheard, S. Y. Yong, and J. Teague. Cosmic: a curated database of somatic variants and clinical data for cancer. *Nucleic Acids Research*, 52:D1210–D1217, 1 2024. ISSN 0305-1048. doi: 10.1093/NAR/GKAD986. URL <https://dx.doi.org/10.1093/nar/gkad986>.

- [31] J. Su, Y. Lu, S. Pan, A. Murtadha, B. Wen, and Y. Liu. Roformer: Enhanced transformer with rotary position embedding, 2023. URL <https://arxiv.org/abs/2104.09864>.
- [32] E. Wang, S. Schmidgall, P. F. Jaeger, F. Zhang, R. Pilgrim, Y. Matias, J. Barral, D. Fleet, and S. Azizi. Txgemma: Efficient and agentic llms for therapeutics.
- [33] A. Yang, B. Yang, B. Hui, B. Zheng, B. Yu, C. Zhou, C. Li, C. Li, D. Liu, F. Huang, G. Dong, H. Wei, H. Lin, J. Tang, J. Wang, J. Yang, J. Tu, J. Zhang, J. Ma, J. Xu, J. Zhou, J. Bai, J. He, J. Lin, K. Dang, K. Lu, K. Chen, K. Yang, M. Li, M. Xue, N. Ni, P. Zhang, P. Wang, R. Peng, R. Men, R. Gao, R. Lin, S. Wang, S. Bai, S. Tan, T. Zhu, T. Li, T. Liu, W. Ge, X. Deng, X. Zhou, X. Ren, X. Zhang, X. Wei, X. Ren, Y. Fan, Y. Yao, Y. Zhang, Y. Wan, Y. Chu, Y. Liu, Z. Cui, Z. Zhang, and Z. Fan. Qwen2 technical report. *arXiv preprint arXiv:2407.10671*, 2024.
- [34] A. Yang, B. Yang, B. Zhang, B. Hui, B. Zheng, B. Yu, C. Li, D. Liu, F. Huang, H. Wei, H. Lin, J. Yang, J. Tu, J. Zhang, J. Yang, J. Yang, J. Zhou, J. Lin, K. Dang, K. Lu, K. Bao, K. Yang, L. Yu, M. Li, M. Xue, P. Zhang, Q. Zhu, R. Men, R. Lin, T. Li, T. Xia, X. Ren, X. Ren, Y. Fan, Y. Su, Y. Zhang, Y. Wan, Y. Liu, Z. Cui, Z. Zhang, and Z. Qiu. Qwen2.5 technical report. *arXiv preprint arXiv:2412.15115*, 2024.
- [35] Q. Zhang, K. Ding, T. Lyv, X. Wang, Q. Yin, Y. Zhang, J. Yu, Y. Wang, X. Li, Z. Xiang, K. Feng, X. Zhuang, Z. Wang, M. Qin, M. Zhang, J. Zhang, J. Cui, T. Huang, P. Yan, R. Xu, H. Chen, X. Li, X. Fan, H. Xing, and H. Chen. Scientific large language models: A survey on biological and chemical domains. *A Survey on Biological and Chemical Domains*, 1:90, 1 2024. doi: 10.1145/nnnnnnnnnnnnnnnn. URL <https://arxiv.org/pdf/2401.14656v2.pdf>.
- [36] Z. Zhou, Y. Ji, W. Li, P. Dutta, R. V. Davuluri, and H. Liu. Dnabert-2: Efficient foundation model and benchmark for multi-species genome. *12th International Conference on Learning Representations, ICLR 2024*, 6 2023. URL <https://arxiv.org/pdf/2306.15006.pdf>.

## A Training Details

### A.1 Hyper-Parameters

All experiments share the following base settings unless otherwise noted. Please look at our GitHub (<https://github.com/bowang-lab/BioReason>) for all other details and training scripts.

- **Optimizer & regularization:**

- Optimizer: AdamW
- Learning rate:  $5 \times 10^{-5}$
- Weight decay:  $1 \times 10^{-2}$
- Gradient accumulation: 8 steps
- Random seed: 23

- **LoRA adapters:**

- Rank: 32
- Alpha: 64
- Dropout: 0.05
- `text_model_finetune`: True
- `dna_model_finetune`: False

- **DeepSpeed & hardware:**

- Strategy: `deepspeed_stage_2`
- GPUs per job: 1
- CPUs per task: 8
- RAM per node: 128–256 GB
- Data-loader workers: 4

- **Task-specific settings:**

- *KEGG pathway reasoning*:
  - Batch size: 1
  - Epochs: 5
  - Max length DNA: 2048
  - Max text length: 1024 (for LLM only increases to 8192 to fit the raw DNA sequences)
- *Variant effect prediction (coding & non-SNV)*:
  - Batch size: 2
  - Epochs: 3
  - Max length DNA: 2048
  - Max text length: 1024 (for LLM only increases to 8192 to fit the raw DNA sequences)

### A.2 Computational Resources

We conducted experiments using multiple GPU clusters equipped with NVIDIA A100 and H100 GPUs. A100 systems were equipped with Intel Xeon Silver CPUs, featuring 16-24 CPU cores, 24-32 threads, and 188-251 GB of RAM. We used 4 A100 GPUs for reinforcement learning, while other experiments were performed on single H100 GPUs with Slurm-based orchestration and DeepSpeed for efficient distributed fine-tuning.

### A.3 Reward Details

We use a composite reward function adapted from [6] to guide reinforcement learning with GRPO, encouraging correctness, format adherence, and brevity. Rewards are assigned deterministically based on post-processed completions. All completions are parsed using a custom XML-aware extractor that isolates final answers from generated reasoning traces, specifically extracting the segment following the final `</think>` tag. The total reward  $r_i$  for each output is the sum of the following components:

- **Correctness Reward.** Assigns a reward of 2.0 if the extracted final answer contains the correct answer (case-insensitive substring match), and 0.0 otherwise.
- **Conciseness Reward.** Adds 0.5 if the extracted answer contains four or fewer words, encouraging brevity in final responses and preventing loopholes around the correctness reward.
- **Strict Format Reward.** Assigns 0.5 if the entire completion matches a strict pattern with a single `<think>` block followed by a final answer line, with newline-separated segments and correct opening/closing tags.
- **Soft Format Reward.** Adds 0.5 if the completion loosely matches the expected `<think>...</think>` format, allowing more relaxed token spacing or structure.
- **Tag Count Reward.** Adds up to 0.25 based on whether exactly one `<think>` and one `</think>` tag are present, with 0.125 points awarded for each.

Each reward component is computed independently and summed per sample. The reward signal is not learned or differentiable, and is used solely within the GRPO training loop to compute group-normalized advantages.

### A.4 GRPO Details

Formally, given an input query  $X_{\text{LLM}}$ , GRPO samples a set of  $G$  outputs  $\{o_1, \dots, o_G\}$  from the current policy  $\pi_{\theta_{\text{old}}}$ . Each candidate output  $o_i$  comprises a reasoning trace and a final response. Outputs are evaluated using a composite domain-specific reward function  $r(q, o_i)$ , incorporating the rewards from Appendix A.3. Broadly:

- **Correctness reward.** We reward accurate final answers extracted from generated outputs.
- **Format adherence reward.** We incentivize compliance with structured output formats, specifically the use of XML-like `<think>` tags for reasoning steps.

GRPO normalizes these rewards into an advantage using the average and standard deviation:

$$A_i = \frac{r_i - \text{mean}(\{r_1, \dots, r_G\})}{\text{std}(\{r_1, \dots, r_G\})} \quad (3)$$

The policy parameters  $\theta$  are then optimized by maximizing the clipped surrogate objective:

$$\begin{aligned} \mathcal{J}_{\text{GRPO}}(\theta) &= \mathbb{E}[X_{\text{LLM}} \sim P(Q), \{o_i\}_{i=1}^G \sim \pi_{\theta_{\text{old}}}(O|X_{\text{LLM}})] \\ &\quad \frac{1}{G} \sum_{i=1}^G \left( \min \left( \frac{\pi_{\theta}(o_i|X_{\text{LLM}})}{\pi_{\theta_{\text{old}}}(o_i|X_{\text{LLM}})} A_i, \text{clip} \left( \frac{\pi_{\theta}(o_i|X_{\text{LLM}})}{\pi_{\theta_{\text{old}}}(o_i|X_{\text{LLM}})}, 1 - \epsilon, 1 + \epsilon \right) A_i \right) - \beta \mathbb{D}_{\text{KL}}(\pi_{\theta} || \pi_{\text{ref}}) \right) \end{aligned} \quad (4)$$

with hyperparameters  $\epsilon$  and  $\beta$ .